Non-Orthogonal Multiple Access in the Presence of Phase Noise

Alexandros-Apostolos A. Boulogeorgos, *Senior Member, IEEE*, Nestor D. Chatzidiamantis, *Member, IEEE*, and George K. Karagiannidis, *Fellow, IEEE*

***Abstract*— In the present letter, we investigate the impact of phase noise on multi-carrier wireless systems that employ non-orthogonal multiple access (NOMA). Specifically, we extract novel closed-form expressions for the outage probability. These expressions can quantify and evaluate the system performance for the general case in which different levels of inter-carrier interference (ICI) is experienced by neighbor carriers as well as the special case, where the neighbor carriers creates the same ICI. The results reveal the importance of taking into consideration the influence of local oscillator imperfections, when assessing the performance of NOMA networks.**

***Index Terms*— Multi-carrier systems, non-orthogonal multiple access, outage probability, phase noise.**

I. Introduction

THE increasing number of data-rate-hungry internet applications has drastically raised the need for high spectral-efficiency and massive connectivity on the next generation wireless networks [1]. In this sense, non-orthogonal multiple access (NOMA) was introduced as an effective approach that enables the simultaneous exploitation of the same frequency resources by multiple users via power-domain multiplexing, while successive interference cancellation (SIC) is implemented in order to eliminate the resulting multi-user interference [2]. As a consequence, a great amount of effort has been put to provide the mathematical framework that quantifies its performance and can be used for design purposes [2], [3]. Additionally, multi-carrier NOMA has been discussed in several published works, including [2], [4], due to its reduced system complexity. In more detail, in single-carrier NOMA, the user with the best channel needs to decode all the other users' signals, which results the high-complexity and decoding delay. On the other hand, in multi-carrier NOMA, the number of users at each carrier is limited; hence, overloading is realized at reduced complexity. In practical implementation, such systems employ direct conversion transceivers, which suffer from radio frequency (RF) front-end (FE) associated impairments, such as in-phase and quadrature-phase imbalance (IQI), power amplifier nonlinearities, and phase noise (PHN) [5]–[8].

Manuscript received February 7, 2020; revised February 21, 2020; accepted February 27, 2020. Date of publication March 6, 2020; date of current version May 8, 2020. The associate editor coordinating the review of this letter and approving it for publication was L. Li. *(Corresponding author: Nestor D. Chatzidiamantis.)*

Alexandros-Apostolos A. Boulogeorgos is with the Department of Electrical and Computer Engineering, Aristotle University of Thessaloniki, 541 24 Thessaloniki, Greece, and also with the Department of Digital Systems, University of Piraeus, 185 34 Piraeus, Greece (e-mail: al.boulogeorgos@ieee.org).

Nestor D. Chatzidiamantis and George K. Karagiannidis are with the Department of Electrical and Computer Engineering, Aristotle University of Thessaloniki, 541 24 Thessaloniki, Greece (e-mail:nestoras@auth.gr; geokarag@auth.gr).

Digital Object Identifier 10.1109/LCOMM.2020.2978845

Scanning the technical literature, the performance of NOMA systems was evaluated in several published papers [9]–[11]. In more detail, in [9], the authors derived the outage probability (OP) and the ergodic capacity of a cooperative NOMA network, in which the nearest user is employed a decode-and-forward relay that is able to switch between full-duplex and half-duplex mode to assist a far user. Likewise, in [10], analytical expressions for the capacity and sum rate of a downlink non-regenerative massive multi-input-multi-output NOMA relay system were presented, whereas, in [11], the authors assessed the outage performance of cloud radio access networks with NOMA. Finally, in [4], a power allocation strategy for multi-carrier NOMA systems was reported.

Despite the negative influence of RF FE imperfections on the system performance of multi-carrier systems [12], they are often ignored, when multi-carrier NOMA is used. In this sense, in [13], the authors investigated the impact of the IQI to downlink multi-carrier NOMA, in terms of the OP. Moreover, in [14] and [15], the authors modeled the aggregated impact of residual hardware imperfections in cooperative wireless systems as an independent and identically distributed additive Gaussian noise and quantified it. The results of all the aforementioned works revealed that hardware imperfections can significantly constraint the system's reliability. Motivated by this as well as the fact that the effect of local oscillator's PHN has not yet been addressed, in this letter, we quantify its effects, in terms of outage performance. In particular, the contribution of this letter can be summarized as follows:

- A novel signal model, which describes the impact of PHN in downlink power-domain NOMA networks is presented. This model is algebraically tractable. Note that, in contrast with IQI [13], which creates interference from a single-carrier, PHN generates interference from multiple neighbor carriers. As a result, both the system model and analysis differ.
- We derive novel closed-form expressions for the OP of multi-carrier systems that employ NOMA as well as the corresponding ones with OMA, in the presence of PHN.

Notations: Unless otherwise stated, $|\cdot|$ denotes the absolute value, while the operators $\exp(\cdot)$, $\log(\cdot)$, and $\log_2(\cdot)$ respectively represent the exponential and the base 10 and 2 logarithmic functions. Likewise, $\sin(x)$, $\cot(x)$ and $\tan^{-1}(x)$ return respectively the sine, cotangent, and arc tangent of x. Moreover, $U(\cdot)$ and $\mathrm{sign}(\cdot)$ respectively stand for the step and sign functions.

II. System & Signal Model

We consider the case of downlink multi-carrier transmission with K RF carriers, in which power-domain NOMA is employed by a base-station (BS) in order to serve M user equipments (UEs) at the same timeslot and in the same

carrier. The fundamental concept behind NOMA is to use superposition coding at the transmitter (TX) and SIC at the receiver (RX). It is also assumed that the RF FE of the BS is ideal, while the UE suffers from PHN. Finally, perfect channel state information is assumed for both the BS and the UEs.

Suppose an information signal intended for UE $i \in U$ with $U = \{1, \cdots, M\}$ through carrier $k \in S$ with $S = \left\{-\frac{K}{2}, \cdots, -1, 1, \cdots, \frac{K}{2}\right\}$, $s_i(k) \in \mathbb{C}$, is carried over a flat-fading channel, $h_i(k) \in \mathbb{C}$, with additive noise $n_i \in \mathbb{C}$. Based on NOMA approach, the baseband equivalent transmitted signal can be modeled as $x(k) = \sum_{i=1}^{M} \sqrt{P_i(k)} s_i(k)$, where $P_i(k)$ stands for the power of the symbol $s_i(k)$. Likewise, the baseband equivalent received signal at the UE i in the carrier k can be obtained as

$$y_i(k) = \xi_i(k) h_i(k) x(k) + z_i(k) + n_i(k), \tag{1}$$

where $h_i(k)$ and $n_i(k)$ are zero mean complex Gaussian processes with variances σ^2 and N_0, respectively, while $\xi_i(k)$ represents the common phase error (CPE) due to PHN, and $z_i(k)$ stands for the inter carrier interference (ICI) caused in the RX, due to PHN. According to [16] and [17], the ICI term can be approximated as

$$z_i(k) \approx \zeta_i h_i(k-1) x(k-1) + \zeta_i h_i(k+1) x(k+1), \tag{2}$$

with $\zeta_i = \exp(j\phi_i(n))$ and $\phi_i(n)$ being the $n-$th sample at the $i-$th UE of a discrete Brownian error process, i.e., $\phi_i(n) = \sum_{m=1}^{n} \phi_i(m-1) + \epsilon_i(n)$, where $\epsilon_i(n)$ is a zero-mean real Gaussian process with variance $\sigma^2_{\epsilon,i} = \frac{4\pi\beta_i}{W}$ and β_i is the LO 3dB bandwidth at the $i-$th UE, whereas W is the wideband channel bandwidth.

Remark 1: From (1) *and* (2)*, it is evident that the level of ICI at carrier k depends not only from the level of imperfections of the RX local oscillator (LO), but also from the total transmitted power at carriers $k+1$ and $k-1$.*

III. Performance Analysis

This section is devoted in analyzing the performance of conventional downlink NOMA in the presence of LO imperfections. Without loss of generality, it is assumed that the channels at carrier k are sorted as $|\tilde{h}_1(k)|^2 \leq |\tilde{h}_2(k)|^2 \leq \cdots \leq |\tilde{h}_M(k)|^2$, where $|\tilde{h}_i(k)|$, $i \in [1, N]$, represents the $i-$th sorted channel gain. According to the NOMA principle, the transmitted power are sorted as $\tilde{P}_1(k) \geq \tilde{P}_2(k) \geq \cdots \geq \tilde{P}_M(k)$, where $\tilde{P}_i(k)$ denotes the transmitted by the $i-$th UE power.[1]

The $m-$th sorted UE performs SIC, by detecting and removing the $i-$th sorted UE's message, with $i < m$, from its observation. As a result, the achievable data rate to the $m-$th sorted UE, $m \in \{1, 2, \cdots, N\}$ at carrier k can be written as

$$R_m(k) = \begin{cases} \log_2\left(1 + \dfrac{\tilde{P}_m(k)|\tilde{h}_m(k)|^2}{|\tilde{h}_m(k)|^2 \sum_{l=m+1}^{M} \tilde{P}_l(k) + i_m(k) + N_0}\right), \\ \qquad m \in [1, M-1] \\ \log_2\left(1 + \dfrac{\tilde{P}_m(k)|\tilde{h}_m(k)|^2}{i_m(k) + N_0}\right), \ m = M \end{cases}$$

[1]Note that, since the BS has not prior-knowledge of the UE LO characteristics, the power will be allocated based on the channels' conditions. Moreover, the decoding order of SIC will depend solitary on the channel ordering.

where $i_m(k)$ represents the level of ICI at the $m-$th UE. Based on [16]–[18] and references therein, for practical values of β, the LO imperfections can be modeled as a zero-mean Gaussian process with a variance given by

$$i_m(k) = A_m(k-1)|h_m(k-1)|^2 \sum_{i=1}^{M} P_i(k-1) + A_m(k+1)|h_m(k+1)|^2 \sum_{i=1}^{M} P_i(k+1). \tag{3}$$

In (3),

$$A_m(l) = \frac{|I_m(f_l - f_k + f_{co}) - I_m(f_l - f_k - f_{co})|}{2\pi f_{co}}, \tag{4}$$

where $l \in \{k-1, k+1\}$. Moreover, f_k is the centered normalized frequency of carrier k, and f_{co} is the normalized cut-off frequency of carrier k, which can be expressed as $f_{co} = \frac{W_{sb}}{2W}$, with W_{sb} being the carrier bandwidth. Finally,

$$\begin{aligned} &I_m(f) \\ &= (f_{co} - f)\tan^{-1}(\delta_m \tan(\pi(f_{co} - f))) \\ &\quad + (f_{co} + f)\tan^{-1}(\delta_m \tan(-\pi(f_{co} + f))) \\ &\quad - \frac{(f_{co} + f)\cot(\pi(f_{co} + f)) - (f_{co} - f)\cot(\pi(f_{co} - f))}{\delta_m} \\ &\quad + \frac{\log(|sin(\pi(f_{co} + f))|) + \log(|sin(\pi(f_{co} - f))|)}{\pi\delta_m}, \end{aligned} \tag{5}$$

with $\delta_m = \frac{\exp(-2\pi\beta_m/W)+1}{\exp(-2\pi\beta_m/W)-1}$.

Note that the achievable data rate, given by (3), is conditioned on $R_{i,m}(k) \geq \tilde{R}_i(k)$, where $R_{i,m}(k)$ and $\tilde{R}_i(k)$ represent the achievable and the targeted data rate for the $m-$th UE at carrier k to detect the $i-$th UE's message ($i < m$) at the same carrier, respectively. Furthermore, the rate for the $m-$th UE to detect the $i-$th UE's message at carrier k can be expressed as

$$R_{i,m}(k) = \log_2\left(1 + \frac{\tilde{P}_i|\tilde{h}_m(k)|^2}{|\tilde{h}_m(k)|^2 \sum_{k=i+1}^{M} \tilde{P}_k + i_m + N_0}\right). \tag{6}$$

The following theorem returns the OP of the $m-$th UE at carrier k.

Theorem 1: The OP of the $m-$th UE at carrier k can be expressed as

$$\mathcal{P}_{m,k} = \sum_{i=1}^{2} \sum_{l=m}^{M} \sum_{p=0}^{l} \binom{M}{l} \binom{l}{p} (-1)^p \times \frac{\Xi(i,1)}{b_i \frac{M-l+p}{\sigma^2} \psi_m + 1} \exp\left(-\frac{M-l+p}{\sigma^2} N_0 \psi_m\right), \tag{7}$$

for $\tilde{R}_i(k) \leq \log_2\left(1 + \frac{\tilde{P}_i}{\sum_{l=i+1}^{M} \tilde{P}_l(k)}\right)$, and $\mathcal{P}_{m,k} = 1$, otherwise. In (7)*,*

$$\psi_m = \max_{i=1,\cdots,m} \left(\frac{\gamma_i(k)}{\tilde{P}_i - \gamma_i(k) \sum_{l=i+1}^{M} \tilde{P}_l(k)}\right), \tag{8}$$

$$b_i = A_m(k + (-1)^i) \sum_{i=1}^{M} P_i(k + (-1)^i), \tag{9}$$

and $\Xi(i,1) = -\frac{1}{b_2}\left(\frac{1}{b_i} - \frac{1}{b_{i+(-1)^{i-1}U(i-1)}}\right)^{-1}$. *Moreover,* $\gamma_i(k) = 2^{\tilde{R}_i(k)} - 1$.

Proof: Please refer to the Appendix A. ∎

Theorem 1 quantifies the impact of LO PHN, number of UE, and power allocation, on the outage performance of the m-th UE. In more detail, we observe that as the number of UE increases, the total interference at the m-th UE also increases; hence, the OP increases. Moreover, the outage performance of the $m-$th UE at carrier k depends not only by the power allocation at carrier k, but also from allocated power at carriers $k-1$ and $k+1$ as well as the ICI suppresions capabilities of the $m-$th UE.

The following lemma returns the OP when $b_1 = b_2$. That is the case where the neighbor carriers create the same level of ICI in the $k-$th carrier. Note that this special case is very close to the reality.

Lemma 1: In the special case in which $b_1 = b_2 = b$, the OP can be evaluated as

$$\mathcal{P}_{m,k} = \sum_{l=m}^{M} \sum_{p=0}^{l} \binom{M}{l} \binom{l}{p} \frac{(-1)^p}{\left(\frac{M-1+p}{\sigma^2} b\psi_m + 1\right)^2} \times \exp\left(-\frac{M-1+p}{\sigma^2}\psi_m N_0\right), \quad (10)$$

for $\tilde{R}_i(k) \leq \log_2\left(1 + \frac{\tilde{P}_i}{\sum_{l=i+1}^{M} \tilde{P}_l(k)}\right)$, and $\mathcal{P}_{m,k} = 1$, otherwise.

Proof: Please refer to Appendix B. ∎

From Theorem 1 and Lemma 1 becomes evident that in order to optimize the NOMA system performance, power allocation should take into consideration carriers $k-1$, k, and $k+1$ in all the involved UE.

For the sake of comparison and completeness, Lemma 2 returns the OP of the $m-$th UE at carrier k of an orthogonal multiple access (OMA) system.

Lemma 2: The OP of the $m-$th UE at carrier k of an OMA system can be obtained as

$$\mathcal{P}_{m,k}^{OMA} = 1 - \sum_{i=1}^{2} \frac{Z(i,1)}{\frac{c_i \gamma_{th}}{P_m \sigma^2} + 1} \exp\left(-\frac{\gamma_{th} N_0}{P_m \sigma^2}\right), \quad (11)$$

where $Z(i,1) = -\frac{1}{c_2}\left(\frac{1}{c_i} - \frac{1}{c_{i+(-1)^{i-1}U(i-1)}}\right)^{-1}$ with $c_i = A_m(k+(-1)^i)P_m(k+(-1)^i)$. Moreover, γ_{th} stands for the SNR threshold and is connected with the targeted data rate, r_{th}, through $\gamma_{th} = 2^{r_{th}} - 1$.

Proof: Please refer to Appendix C. ∎

Notice that the OMA network requires M resource blocks to serve the M UE, while the NOMA demands 1. Therefore, for the shake of fair comparison, $r_{th} = M\tilde{R}_m(k)$. Finally, from Lemma 2, we observe that the level of ICI in OMA systems depends on the power allocation in the carriers $k-1$ and $k+1$ of the $m-$th UE.

IV. Results and Discussion

This section focuses on the quantification of the impact of PHN on the outage performance of the NOMA system as well as the verification through Monte Carlo simulations. The following insightful scenario is considered. Unless otherwise stated, $M = 2$, the outage performance at the carrier $k = 4$ in a multicarrier systems consisting of $K = 8$ carriers, is investigated. Moreover, $W_{sb} = 2.23$ MHz, and $W = 2.24$ MHz.

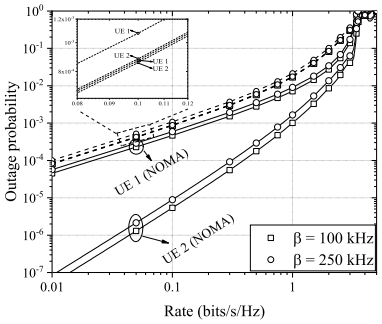

Fig. 1. OP vs $\tilde{R}_m$, for different values of β.

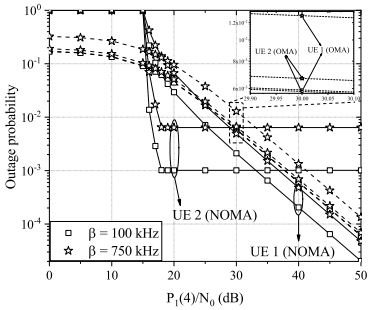

Fig. 2. OP vs $\frac{\tilde{P}_1(4)}{N_0}$, for different values of β.

Finally, we assume that the LO 3-dB bandwidth, β. In the following figures, the numerical results are shown with continuous or/and dashed lines, while markers are employed to illustrate the respective Monte Carlo simulation results.

Fig. 1 plots the OP of both the UE as a function of their targeted rate, for different values of β, assuming $\tilde{P}_1(4)/N_0 = 25$ dB, $P_1(3)/N_0 = 15$ dB, $P_1(5)/N_0 = 5$ dB, $\tilde{P}_2(4)/N_0 = 15$ dB, $P_2(3)/N_0 = 5$ dB, and $P_2(5)/N_0 = 0$ dB. Moreover, as a benchmark, the corresponding outage performance of the OMA system fot both the UEs, assuming that $P_1(4)/N_0 = P_2(4)/N_0 = 1/2\left(\tilde{P}_1(4)/N_0 + \tilde{P}_2(4)/N_0\right)$. In both scenarios, it is assumed that both UE have the same targeted rate. As expected, for both UE and a given β and a specific access scheme, as the targeted rate increases, the OP also increases. Moreover, it is observed that for both UE and for a fixed targeted rate, as LO quality degrades, i.e. as β increases, the OP increases. Additionally, it is evident, that there exists a targeted rate threshold, after which the OP equals 1. Finally, we observe that, in general, independently of β and $\tilde{R}_m$, NOMA outperforms OMA.

Fig. 2 depicts the OP of both UE as a function of $\frac{\tilde{P}_1(4)}{N_0}$, for different values of β, assuming that the targeted rate of both users is 1 bits/s/Hz, $P_1(3)/N_0 = 15$ dB, $P_1(5)/N_0 = 5$ dB, $\tilde{P}_2(4)/N_0 = 15$ dB, $P_2(3)/N_0 = 5$ dB and $P_2(5)/N_0 = 0$ dB. Again, as a benchmark, the performance of both UE in the corresponding OMA system is presented. For UE 1 and a fixed β, as $\frac{\tilde{P}_1(4)}{N_0}$ increases, the outage performance improves. Similarly, in NOMA, for UE 2, a given β and $\frac{\tilde{P}_1(4)}{N_0} < \frac{\tilde{P}_2(4)}{N_0}$, as $\frac{\tilde{P}_1(4)}{N_0}$ increases, the OP decreases. On the other hand, for $\frac{\tilde{P}_1(4)}{N_0} > \frac{\tilde{P}_2(4)}{N_0}$, the increase of $\frac{\tilde{P}_1(4)}{N_0}$ does not affect the outage performance of UE 2. Meanwhile, for a given $\frac{\tilde{P}_1(4)}{N_0}$, for both UE, as β increases, the ICI increases; hence, the outage performance degrades. Finally, it is observed that in the low-$P_1(4)/N_0$ regime, where the outage probability of the NOMA equals 1, OMA outperforms NOMA, while in the

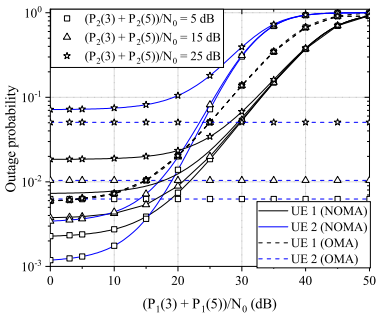

Fig. 3. OP of UE 2 vs $\frac{P_1(3)+P_1(5)}{N_0}$, for different values of $\frac{P_2(3)+P_2(5)}{N_0}$.

medium-$P_1(4)/N_0$ regime, both the UE achieve better outage performance when NOMA is employed instead of OMA. Interestingly, in the high-$P_1(4)/N_o$ regime, although UE 1 can achieve better performance by employing NOMA than OMA, UE 2 achieves a lower outage probability when OMA is employed. This is due to the employed power allocation scheme in NOMA, where $\tilde{P}_2(4)$ is kept constant.

In Fig. 3, the OP of both users is demonstrated as a function of $\frac{P_1(3)+P_1(5)}{N_0}$, for different values of $\frac{P_2(3)+P_2(5)}{N_0}$, assuming that the targeted data rate for both nodes is 0.01 bits/s/Hz, $\frac{P_1(4)}{N_0} = 20$ dB, $\frac{P_2(4)}{N_0} = 10$ dB, and $\beta = 100$ kHz. For a fixed $\frac{P_2(3)+P_2(5)}{N_0}$, as $\frac{P_1(3)+P_1(5)}{N_0}$ increases, i.e., as the inter-carrier interference, which is caused by UE 1, the OP of both UE also increases. Similarly, for a given $\frac{P_1(3)+P_1(5)}{N_0}$, as $\frac{P_2(3)+P_2(5)}{N_0}$ increases, the inter-carrier interference from UE 2 increases; as a results the outage performance degrades. These observations indicate that in order to achieve an outage performance requirement for UE 1 and 2, the power of the neighbor carriers needs to be appropriately allocated. Finally, from this figure, we observe that in general in the low-ICI regime, NOMA outperforms OMA in terms of outage probability. However, in the high-ICI UE employing OMA can achieve better performance compared to the ones that use NOMA. This indicates the importance of taking into account the impact of PHN when selecting the access strategy.

V. Conclusion

In this letter, we studied the impact of UE's LO's imperfections in the performance of a wireless multiple access system, which employs NOMA. In this sense, we presented novel closed-form expressions for the OP that takes into account the power allocation of the neighbor carriers and the level of LOs imperfections of each UE. Our results reveal the importance of taking into account the power allocation of the neighbor carriers and the intensity of PHN, when analyzing and designing such systems. Finally, they highlighted the importance of taking into account the levels of ICI when selecting the access scheme.

Appendixes

Appendix A
Proof of Theorem 1

Assuming that the quality of service requirements are determined by the UEs, an outage event at carrier k at the $m-$th UE can occur when the $m-$th UE is unable to detect its own message or the message intended for the $i-$th UE ($i < m$). Hence, the OP at the $m-$th UE can be obtained as

$$\mathcal{P}_{m,k} = 1 - \Pr\left(\mathcal{U}_{1,m} \cap \cdots \cap \mathcal{U}_{m,m}\right), \tag{12}$$

where $P_r(\mathcal{U})$ stand for the probability that the event $\mathcal{U}$ occurs with $\mathcal{U} = \{\mathcal{U}_{1,m} \cap \cdots \cap \mathcal{U}_{m,m}\}$, and $\mathcal{U}_{i,m} = \left\{R_{i,m}(k) \geq \tilde{R}_i(k)\right\}$.

By substituting (3) and (6) into (12), the OP can be equivalently written as

$$\mathcal{P}_{m,k} = 1 - \Pr\left(\left\{A_{1,m}|\tilde{h}_m(k)|^2 \geq B_{1,m}\right\} \cap \cdots \cap \left\{A_{m,m}|\tilde{h}_m(k)|^2 \geq B_{m,m}\right\}\right), \tag{13}$$

where $A_{i,m} = \tilde{P}_i - \gamma_{i,m}(k)\sum_{l=i+1}^{M}\tilde{P}_l(k)$, and $B_{i,m} = \gamma_{i,m}(k)\left(i_m + N_0\right)$.

By assuming that $A_{i,m} \geq 0$, for $i \in [1, m]$, i.e. $R_{i,m}(k) \leq \log_2\left(1 + \frac{\tilde{P}_i}{\sum_{l=i+1}^{M}\tilde{P}_l(k)}\right)$, (13) can be rewritten as $\mathcal{P}_{m,k} = 1 - \Pr\left(\frac{|\tilde{h}_m(k)|^2}{i_m(k)+N_0} \geq \psi_m\right)$, or

$$\mathcal{P}_{m,k} = \Pr\left(\mathcal{X} \leq \psi_m\right) = F_X(\psi_m), \tag{14}$$

where $F_{\mathcal{X}}(\cdot)$ stands for the cumulative density function (CDF) of the random variable (RV) $\mathcal{X}$, defined as $\mathcal{X} = \frac{|\tilde{h}_m(k)|^2}{i_m(k)+N_0}$. Since $|\tilde{h}_m(k)|^2$ and $i_m(k)$ are independent RVs, (14) can be evaluated as

$$F_X(\psi_m) = \int_{N_0}^{\infty} F_{|\tilde{h}_m|^2}\left(\psi_m x\right) f_{\mathcal{Y}}(x)\mathrm{dx}, \tag{15}$$

where $F_{|\tilde{h}_m|^2}(\cdot)$ and $f_{\mathcal{Y}}(\cdot)$ are the CDF and the probability density function (PDF) of $|\tilde{h}_m|^2$ and the RV $\mathcal{Y} = i_m(k) + N_0$, respectively.

Since $|\tilde{h}_m|$ is an ordered Rayleigh RV, $|\tilde{h}_m|^2$ will be an ordered exponential RV with CDF given by [19]

$$F_{|\tilde{h}_m|^2}(x) = \sum_{l=m}^{M}\sum_{p=0}^{l}\binom{M}{l}\binom{l}{p}(-1)^p \times \exp\left(-\frac{M-l+p}{\sigma^2}x\right). \tag{16}$$

Likewise, since $\mathcal{Y}$ is a shifted weighted-sum of square Rayleigh RVs, its PDF can be obtained as [20]

$$f_{\mathcal{Y}}(x) = \sum_{i=1}^{2}\frac{\Xi(i,1)}{b_i}\exp\left(-\frac{x-N_0}{b_i}\right), \tag{17}$$

where $\Xi(i,1)$ can be obtained as [20, Eqs. (8) and (9)].

By substituting (16) and (17) into (15) and after some mathematical manipulations, we can express the CDF of $\mathcal{X}$ as

$$F_X(\psi_m) = \sum_{i=1}^{2}\sum_{l=m}^{M}\sum_{p=0}^{l}\binom{M}{l}\binom{l}{p}(-1)^p\Xi(i,1) \times \exp\left(\frac{N_0}{b_i}\right)\int_{N_0}^{\infty}\exp\left(-\left(\frac{M-l+p}{\sigma^2}\psi_m + \frac{1}{b_i}\right)x\right)\mathrm{dx}, \tag{18}$$

which, after performing the integration, returns (7).

Next, we examine the case in which $A_{i,m} < 0$. In this case, since $B_{i,m}$ is always non-negative, $\Pr\left(\overline{\mathcal{U}}_{1,m} \cap \cdots \cap \overline{\mathcal{U}}_{m,m}\right) = 0$, where $\overline{\mathcal{U}}_{i,m} = \left\{A_{i,m}|\tilde{h}_m(k)|^2 \geq B_{i,m}\right\}$, with $i = 1, \cdots, m$; hence, $\mathcal{P}_{m,k} = 1$. This concludes the proof.

APPENDIX B
PROOF OF LEMMA 1

In the special case in which $b_1 = b_2 = b$, i_m is the sum of two independent and identical exponential distributed RVs; hence, it follows a Gamma distribution with PDF that can be expressed as

$$f_{i_m}^{sc}(x) = \frac{x}{b^2} \exp\left(-\frac{x}{b}\right). \tag{19}$$

Moreover, the PDF of $\mathcal{Y}$ can be obtained, with the aid of (19), as

$$f_{\mathcal{Y}}^{sc}(x) = \frac{x - N_0}{b^2} \exp\left(-\frac{x - N_0}{b}\right), \text{ with } x \geq N_0. \tag{20}$$

By substituting (20) into (15) and following the same steps as in Appendix A, we can derive the CDF of $\mathcal{X}$ as

$$\begin{aligned} F_{\mathcal{X}}^{sc}(x) &= \sum_{l=m}^{M} \sum_{p=0}^{l} \binom{M}{l} \binom{l}{p} (-1)^p \\ &\quad \times \left(\frac{M-1+p}{\sigma^2} bx + 1\right)^{-2} \exp\left(-\frac{M-1+p}{\sigma^2} x N_0\right). \end{aligned} \tag{21}$$

Likewise, by employing (14), for $R_i(k) \leq \log_2\left(1 + \frac{\sum_{l=i+1}^{M} \tilde{P}_l(k)}{\tilde{P}_i}\right)$, we get (10). Note that in the case in which $R_i(k) > \log_2\left(1 + \frac{\sum_{l=i+1}^{M} \tilde{P}_l(k)}{\tilde{P}_i}\right)$, we can prove by following the same steps as Appendix A that $P_{m,k}^{sc} = 1$.

APPENDIX C
PROOF OF LEMMA 2

The OP of the $m-$th UE at carrier k in the OMA system can be defined as

$$\mathcal{P}_{m,k}^{(\text{OMA})} = \Pr\left(R_m^{(\text{OMA})}(k) \leq r_{th}\right), \tag{22}$$

where $R_m^{(\text{OMA})}(k)$ is the achievable data rate in the carrier k of the $m-$th UE and can be obtained as $R_m^{(\text{OMA})}(k) = \log_2\left(1 + \frac{P_m|h_m|^2}{i_m + N_0}\right)$. By following the same steps as Appendix A, we can rewrite (22) as

$$\mathcal{P}_{m,k}^{(\text{OMA})} = \int_{N_0}^{\infty} F_{|h_m|^2}\left(\frac{\gamma_{th}}{P_m} x\right) f_{\mathcal{Y}_1}(x)\, \mathrm{dx}, \tag{23}$$

where is the CDF of $|h_m|^2|$ and $f_{\mathcal{Y}_1}(x)$ is the PDF of $\mathcal{Y}_1 = A_m(k-1)|h_m(k-1)|^2 + A_m(k+1)|h_m(k+1)|^2 + N_0$. Of note, since $|h_m|$ is a Rayleigh distributed RV, $|h_m|^2$ is exponential distributed; thus, its CDF can be obtained as

$$F_{|h_m|^2}(x) = 1 - \exp\left(-\frac{x}{\sigma^2}\right). \tag{24}$$

Moreover, $\mathcal{Y}_1$ is a shifted squared Rayleigh RV; hence, its PDF can be obtained as

$$f_{\mathcal{Y}_1}(x) = \sum_{i=1}^{2} \frac{Z(i,1)}{c_i} \exp\left(-\frac{x - N_0}{c_i}\right). \tag{25}$$

By substituting (24) and (25) into (23) and performing the integration, we derive (11). This concludes the proof.

REFERENCES

[1] Y. Liu, Z. Ding, M. Elkashlan, and H. V. Poor, "Cooperative non-orthogonal multiple access with simultaneous wireless information and power transfer," *IEEE J. Sel. Areas Commun.*, vol. 34, no. 4, pp. 938–953, Apr. 2016.

[2] Z. Ding, X. Lei, G. K. Karagiannidis, R. Schober, J. Yuan, and V. K. Bhargava, "A survey on non-orthogonal multiple access for 5G networks: Research challenges and future trends," *IEEE J. Sel. Areas Commun.*, vol. 35, no. 10, pp. 2181–2195, Oct. 2017.

[3] Y. Liu, Z. Qin, M. Elkashlan, Z. Ding, A. Nallanathan, and L. Hanzo, "Nonorthogonal multiple access for 5G and beyond," *Proc. IEEE*, vol. 105, no. 12, pp. 2347–2381, Dec. 2017.

[4] W. Xu, X. Li, C.-H. Lee, M. Pan, and Z. Feng, "Joint sensing duration adaptation, user matching, and power allocation for cognitive OFDM-NOMA systems," *IEEE Trans. Wireless Commun.*, vol. 17, no. 2, pp. 1269–1282, Feb. 2018.

[5] A.-A.-A. Boulogeorgos, V. M. Kapinas, R. Schober, and G. K. Karagiannidis, "I/Q-imbalance self-interference coordination," *IEEE Trans. Wireless Commun.*, vol. 15, no. 6, pp. 4157–4170, Jun. 2016.

[6] E. Bjornson, M. Matthaiou, and M. Debbah, "Massive MIMO systems with hardware-constrained base stations," in *Proc. IEEE Int. Conf. Acoust., Speech Signal Process. (ICASSP)*, May 2014, pp. 3142–3146.

[7] E. Bjornson, M. Matthaiou, and M. Debbah, "A new look at dual-hop relaying: Performance limits with hardware impairments," *IEEE Trans. Commun.*, vol. 61, no. 11, pp. 4512–4525, Nov. 2013.

[8] J. Li, M. Matthaiou, and T. Svensson, "I/Q imbalance in AF dual-hop relaying: Performance analysis in Nakagami-m fading," *IEEE Trans. Commun.*, vol. 62, no. 3, pp. 836–847, Mar. 2014.

[9] X. Yue, Y. Liu, S. Kang, A. Nallanathan, and Z. Ding, "Exploiting full/half-duplex user relaying in NOMA systems," *IEEE Trans. Commun.*, vol. 66, no. 2, pp. 560–575, Feb. 2018.

[10] D. Zhang, Y. Liu, Z. Ding, Z. Zhou, A. Nallanathan, and T. Sato, "Performance analysis of non-regenerative Massive-MIMO-NOMA relay systems for 5G," *IEEE Trans. Commun.*, vol. 65, no. 11, pp. 4777–4790, Nov. 2017.

[11] X. Gu, X. Ji, Z. Ding, W. Wu, and M. Peng, "Outage probability analysis of non-orthogonal multiple access in cloud radio access networks," *IEEE Commun. Lett.*, vol. 22, no. 1, pp. 149–152, Jan. 2018.

[12] T. Schenk, *RF Imperfections in High-Rate Wireless Systems: Impact and Digital Compensation*. The Netherlands: Springer, 2008.

[13] B. Selim *et al.*, "Performance analysis of non-orthogonal multiple access under I/Q imbalance," *IEEE Access*, vol. 6, pp. 18453–18468, 2018.

[14] F. Ding, H. Wang, S. Zhang, and M. Dai, "Impact of residual hardware impairments on non-orthogonal multiple access based Amplify-and-Forward relaying networks," *IEEE Access*, vol. 6, pp. 15117–15131, 2018.

[15] X. Li, J. Li, Y. Liu, Z. Ding, and A. Nallanathan, "Residual transceiver hardware impairments on cooperative noma networks," *IEEE Trans. Wireless Commun.*, vol. 19, no. 1, pp. 680–695, Jan. 2020.

[16] A. Gokceoglu, Y. Zou, M. Valkama, and P. C. Sofotasios, "Multi-channel energy detection under phase noise: Analysis and mitigation," *Mobile Netw. Appl.*, vol. 19, no. 4, pp. 473–486, Aug. 2014.

[17] A.-A.-A. Boulogeorgos, N. D. Chatzidiamantis, and G. K. Karagiannidis, "Energy detection spectrum sensing under RF imperfections," *IEEE Trans. Commun.*, vol. 64, no. 7, pp. 2754–2766, Jul. 2016.

[18] A.-A. A. Boulogeorgos, "Interference mitigation techniques in modern wireless communication systems," Ph.D. dissertation, Aristotle Univ. Thessaloniki, Thessaloniki, Greece, Sep. 2016.

[19] H. David and H. N. Nagaraja, *Order Statist.* (Wiley Series in Probability and Statistics). Hoboken, NJ, USA: Wiley, 2004.

[20] G. K. Karagiannidis, N. C. Sagias, and T. A. Tsiftsis, "Closed-form statistics for the sum of squared Nakagami-m variates and its applications," *IEEE Trans. Commun.*, vol. 54, no. 8, pp. 1353–1359, Aug. 2006.